THE BLAST FROM A SPHERE OF HIGH PRESSURE GAS

by

H. L. Brode

P-582

January 27, 1955

The RAND Corporation
1700 MAIN ST. • SANTA MONICA • CALIFORNIA

ABSTRACT

The gas dynamics resulting from the release of an isothermal sphere of gas initially at rest and at a high pressure are described by the numerical solution of the differential equations which represent an ideal gas in radial motion. The resulting outward shock and the inward rarefactions and shocks are described in some detail and are compared with the gas dynamics of the point-source solution.[1] The existence of the inward moving shocks has been discussed in several places[2-4] and in one instance the early phase has been numerically calculated.[5] This phenomenon is observed in the present calculations to occur repeatedly, subjecting the origin to several compressive waves which are reflected there and which move out to overtake the main shock.

---

[1] H. L. Brode, Phys. Rev. 95, 658 (A) (1954).

[2] F. Wecken, Z. angew, Math. Mech. 30, 270 (1950).

[3] J. A. McFadden, J. Appl. Phys. 23, 1269 (1952).

[4] H. Schardin, Communications on Pure and Applied Mathematics (Inst. of Mathematical Sciences, New York University, (1954), Vol. VII, p. 223.

[5] T. S. Walton, Phys. Rev. 87, 910 (A) (1952).

THE BLAST FROM A SPHERE OF HIGH PRESSURE GAS*

I have used a method proposed in 1950 by von Neumann and Richtmyer[1] for numerically integrating the differential equations of state and motion of an ideal gas. The method introduces an artificially large viscosity for the purpose of avoiding shock discontinuities in the numerics.

I described the blast wave resulting from a point source at the last Washington meeting[2]. These results are also to be published in the Journal of Applied Physics.[3] In this paper I shall not mention the details of the numerical methods but shall describe briefly some interesting features of the blast wave resulting from a finite source, in particular an initially static and isothermal high-pressure sphere.

EQUATIONS OF MOTION

The equations of motion in some units and in Lagrangean form may be expressed as these

$$\frac{\partial \lambda}{\partial x} = \frac{1}{\rho \lambda^2} \quad \text{or} \quad \frac{\partial \rho}{\partial \tau} = -\rho \left(\frac{2u}{\lambda} + \frac{\partial u/\partial x}{\partial \lambda/\partial x} \right) \qquad \text{(mass)}$$

$$\frac{\partial u}{\partial \tau} = \frac{-\lambda^2}{\gamma} \frac{\partial}{\partial x} (P + q) \qquad \text{(momentum)} \qquad (1)$$

$$\frac{\partial P}{\partial \tau} = \frac{1}{\rho} \frac{\partial \rho}{\partial \tau} \times \left[\gamma P + (\gamma - 1) q \right] \qquad \text{(energy)}$$

In which λ is a reduced radial distance, x is the mass or Lagrangean

---

* Presented at the American Physical Society Meeting, January 27-29, 1955.

1. von Neumann, J. and Richtmyer, R. D., J. Appl. Phys. 21, 232 (1950)

2. Brode, H. L., Numerical Solution of a Spherical Blast Wave, Phys.Rev. 95, 658(A)

3. Brode, H. L., Journal Appl. Phys. (to be published)

coordinate, τ is the time coordinate and ρ, P, u, q, are respectively the density, pressure, particle velocity, and artificial viscosity in units of some ambient values. For this problem gamma was taken to be that of normal air (1.4).

The particular form used for the artificial viscosity is the following:

$$q = \frac{9\gamma(\gamma+1)}{4}\left(\frac{M}{3\pi}\right)^2 \rho(\Delta x)^2 \left(\frac{\partial u}{\partial x}\right)\left(\frac{\partial u}{\partial x} - \left|\frac{\partial u}{\partial x}\right|\right)$$

M = Number of zones spread (2)

$$\lambda = r/\epsilon$$

$$\epsilon^3 = \frac{E_{tot}}{P_o} = \frac{4\pi}{P_o}\int_o^R \rho\left(E_{int} + \frac{u^2}{2}\right) r^2 dr$$

This form has the property that it is zero except for compressions, i.e., shocks, where it spreads the shock over a constant number of space zones (M). The reduced radius (λ) is shown to be dimensionless and related to the total blast energy (E_{tot}) and the ambient or pre-shock pressure (P_o).

DIFFERENCE EQUATIONS

We approximate the differential equations by the following difference equations, and, beginning with a particular set of initial conditions, advance a problem in n steps of $\Delta\tau$ over a mesh of ℓ, Δx in accordance with stability and accuracy requirements.

$$u_\ell^{\,n+\frac{1}{2}} = u_\ell^{\,n-\frac{1}{2}} - \frac{\Delta\tau(\lambda_\ell^{\,n})^2}{(\Delta x)_\ell \gamma}\left[P_{\ell+\frac{1}{2}}^{\,n} - P_{\ell-\frac{1}{2}}^{\,n} + q_{\ell+\frac{1}{2}}^{\,n-\frac{1}{2}} - q_{\ell-\frac{1}{2}}^{\,n-\frac{1}{2}}\right]$$

$$\lambda_\ell^{\,n+1} = \lambda_\ell^{\,n} + u_\ell^{\,n+\frac{1}{2}}\,\Delta\tau$$

$$W = \Delta\tau\left(\frac{2(u_\ell^{\,n+\frac{1}{2}} + u_{\ell-1}^{\,n+\frac{1}{2}})}{\lambda_\ell^{\,n+1} + \lambda_\ell^{\,n} + \lambda_{\ell-1}^{\,n+1} + \lambda_{\ell-1}^{\,n}} + \frac{u_\ell^{\,n+\frac{1}{2}} - u_{\ell-1}^{\,n+\frac{1}{2}}}{\lambda_\ell^{\,n+1} + \lambda_\ell^{\,n} - \lambda_{\ell-1}^{\,n+1} - \lambda_{\ell-1}^{\,n}}\right) \quad (3)$$

$$\rho_{\ell-\frac{1}{2}}^{n+1} = \rho_{\ell-\frac{1}{2}}^{n}\left(\frac{1-W}{1+W}\right)$$

$$q_{\ell-\frac{1}{2}}^{n+\frac{1}{2}} = 9\,\frac{\gamma(\gamma+1)}{2}\left(\frac{M}{3\pi}\right)^2 \rho_{\ell-\frac{1}{2}}^{n+1}\left[u_{\ell-1}^{n+\frac{1}{2}} - u_{\ell-1}^{n+\frac{1}{2}}\right]^2$$

M = number of zones shock spread (e.g. 6)

$$\text{for } u_{\ell-1} > u_{\ell} \tag{4}$$

$$q_{\ell-\frac{1}{2}}^{n+\frac{1}{2}} = 0 \qquad \text{for } u_{\ell-1} \leqslant u_{\ell}$$

$$P_{\ell-\frac{1}{2}}^{n+1} = \frac{\left[\frac{(\gamma+1)}{(\gamma-1)}\rho_{\ell-\frac{1}{2}}^{n+1} - \rho_{\ell-\frac{1}{2}}^{n}\right] P_{\ell-\frac{1}{2}}^{n} + 2\left(\rho_{\ell-\frac{1}{2}}^{n+1} - \rho_{\ell-\frac{1}{2}}^{n}\right) q_{\ell-\frac{1}{2}}^{n+\frac{1}{2}}}{\frac{(\gamma+1)}{(\gamma-1)}\rho_{\ell-\frac{1}{2}}^{n} - \rho_{\ell-\frac{1}{2}}^{n+1}}$$

The main feature of each problem is the outward-moving shock. Fig. 1 compares the shock overpressure originating from two isothermal spheres, one initially at 121 atmospheres, the other at 2003 atmospheres, with a point-source solution (started from an analytical form valid for strong shocks and due to Taylor or von Neumann.[4]) The isothermal spheres were at normal density originally and consequently were also at a high temperature. In all cases the finite source curve becomes indistinguishable from the point source curve after the shock from the isothermal sphere has engulfed a mass of air ten times the initial mass.

A cold source was run in which the same initial pressure was used but the temperature was initially equal inside and out, which meant a high initial density. In this case the overpressure did not rise to the point-source value until quite late when it had fallen to about a half an atmosphere. At that point, however, the mass engulfed was again approximately ten times the

---

4. AECD-28060 "Shock Hydrodynamics and Blast Waves," Los Alamos Scientific Laboratory, 28 October 1944.

initial mass.

Fig. 2 shows some pressure profiles as a function of the radius at various early times after release of an isothermal sphere of normal density gas at two thousand atmos initial pressure. Note development of the outward shock and the inward rarefaction. Note in particular the development of an inward shock following the rarefaction. This shock does not attain a net inward motion until the rarefaction has "reflected" at the origin.

In Fig. 3 we view pressure-radius profiles near the center and at times just before and after this inward shock impinges on the origin. Arrows indicate the general movement with time and hence the sequence for nearly constant time-intervals.

Since the shocks are, of necessity, spread over several mesh points, the picture near a singular point such as the origin appears quite smeared out with a consequent loss of detail.

Using mesh sizes about one fourth the original size, portions of the problem were re-run. Admitting some uncertainty in positions and peak values of shocks, a comparison of the shock pressure for this inward moving shock shows some appreciable discrepancy only near the origin. After reflection the discrepancy decreases again in spite of their quite different histories near the center. The discrepancy may be attributed mainly to the difficulty in identifying the shock when the rounding is comparable to the shock radius.

This shock pressure is decreasing initially although moving inward since the net outward expansion behind the main shock is dominant. (Fig. 4).

If one considers rather than the absolute pressure, the ratio of excess shock pressure over the pressure immediately in front of the shock, a quantity more characteristic of the strength of this shock, then it is seen that the inward shock is increasing in strength but remains stationary until its pressure ratio is greater than unity. (Fig. 5).

The reflected shock moves into a higher pressure and so has a lower ratio.

The reflected shock decreases about inversely with the radial distance although it has a finite strength.

The density profiles at early times show a sharp compression spike at the main shock and a rarefaction eating inward from the surface of the initial sphere. (Fig. 6). The rarefaction reduces the density in the sphere to a very low value. The inward shock is seen to reflect and move outward, overtake the main shock and leave a permanent discontinuity in density (and temperature) at the point of coalescence.

The temperature profiles at early times (Fig. 7), show the cooling effect of the rarefaction and the very modest heating done by the main shock. Just as with the density a sharp break or discontinuity is maintained at the boundary of the initially heated sphere. The inward shock is seen in even greater contrast here.

The dotted curve indicates the results with a smaller mesh size at the same time as the dashed curve which is for a larger mesh size.

After some considerable time two similar problems with considerably different zone sizes compare about as in Fig. 8.

The portion near the origin was covered with a fine grid in the case illustrated by the dashed curve. The grid was coarser for the same case near the main shock, however, which accounts for the poor reproduction of the second shock at this point high on the back of the main shock.

In addition to the main shock and the inward shock shown previously, successively smaller shocks develop from interaction with the contact discontinuity at the edge of the initial sphere. This boundary is marked by ticks in Fig. 9. Note the reflected and the transmitted shocks being formed.

The initial rarefaction reflects at the origin and on moving outward interacts with this same discontinuity to send back a pulse.

This pulse, in turn, runs into the outward-moving second shock and sends inward a pulse containing elements of both rarefaction and compression. In

this figure, this pulse is shown interacting with the origin. In the upper curve a rarefaction followed by a shock is moving inward. The middle curve shows the rarefaction reflected and the shock still inward bound. The lower curve finds this shock reflected and moving out.

Retracing a little in time, the next set of pressure-profiles (Fig. 10), show the main shock decay with time and the movement of the second shock after reflection at the center. In the second curve this second shock is just passing through the discontinuity, and the minor pulse shown on the previous slide is about to hit the center. In the third curve the second shock is riding up the main shock and a tertiary shock reflected from the interface is racing inward. The fourth curve shows this third shock outward bound.

In the first curve of Fig. 11, the second shock is about to close with the main shock and the third shock is encountering the interface. The second curve shows the first two shocks coalesced and the third shock rising up the main shocks.

Pulses and small shocks rattle back and forth in this hot interior subjecting the origin to repeated shocks and temperature rises, so that the temperature gradient in the gas that started out as isothermal becomes more and more like that of the point source as time goes on.

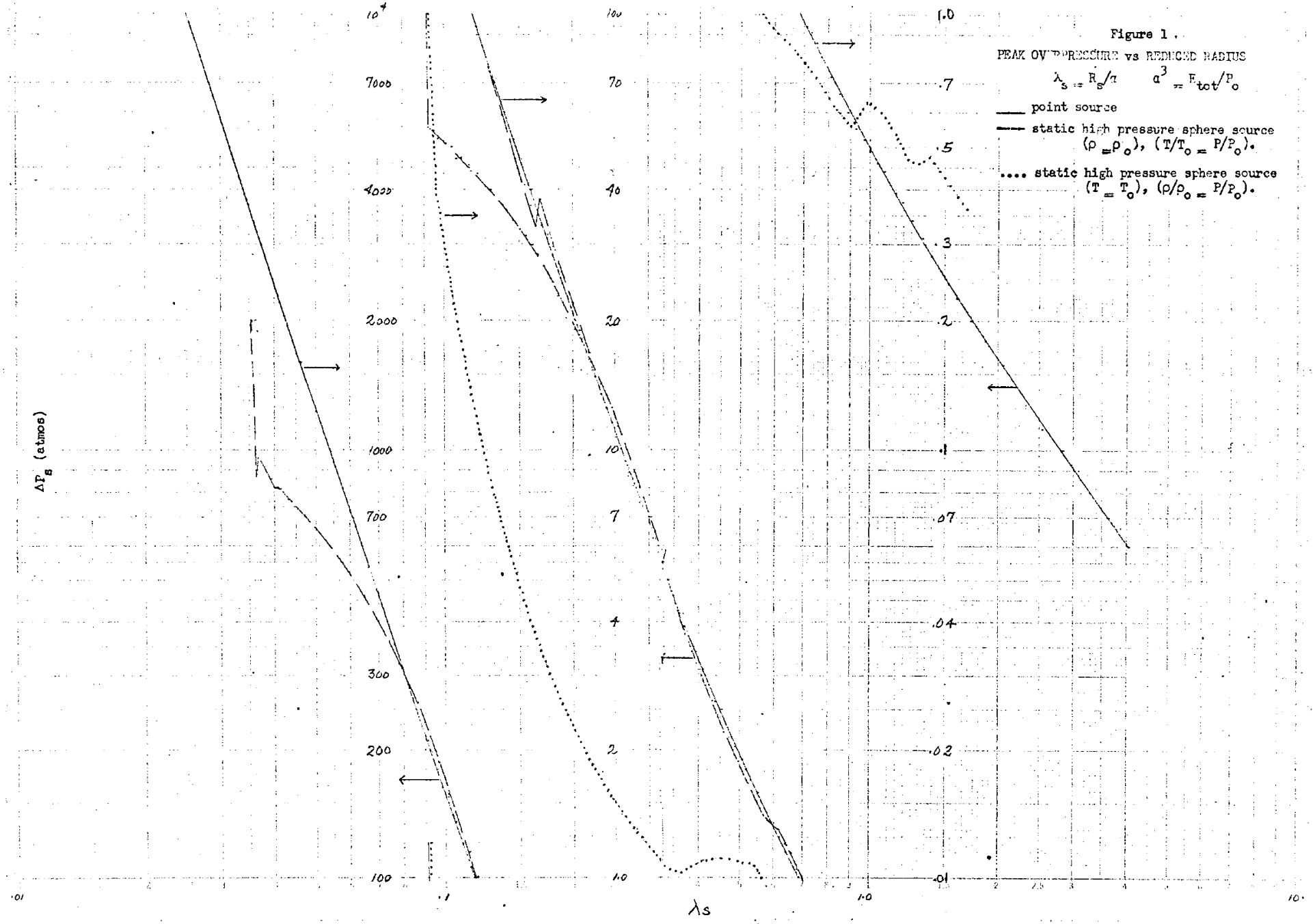

Figure 1.

PEAK OVERPRESSURE vs REDUCED RADIUS

$\lambda_s = R_s/a$ $\quad a^3 = E_{tot}/P_o$

—— point source

—— static high pressure sphere source ($\rho = \rho_o$), ($T/T_o = P/P_o$).

···· static high pressure sphere source ($T = T_o$), ($\rho/\rho_o = P/P_o$).

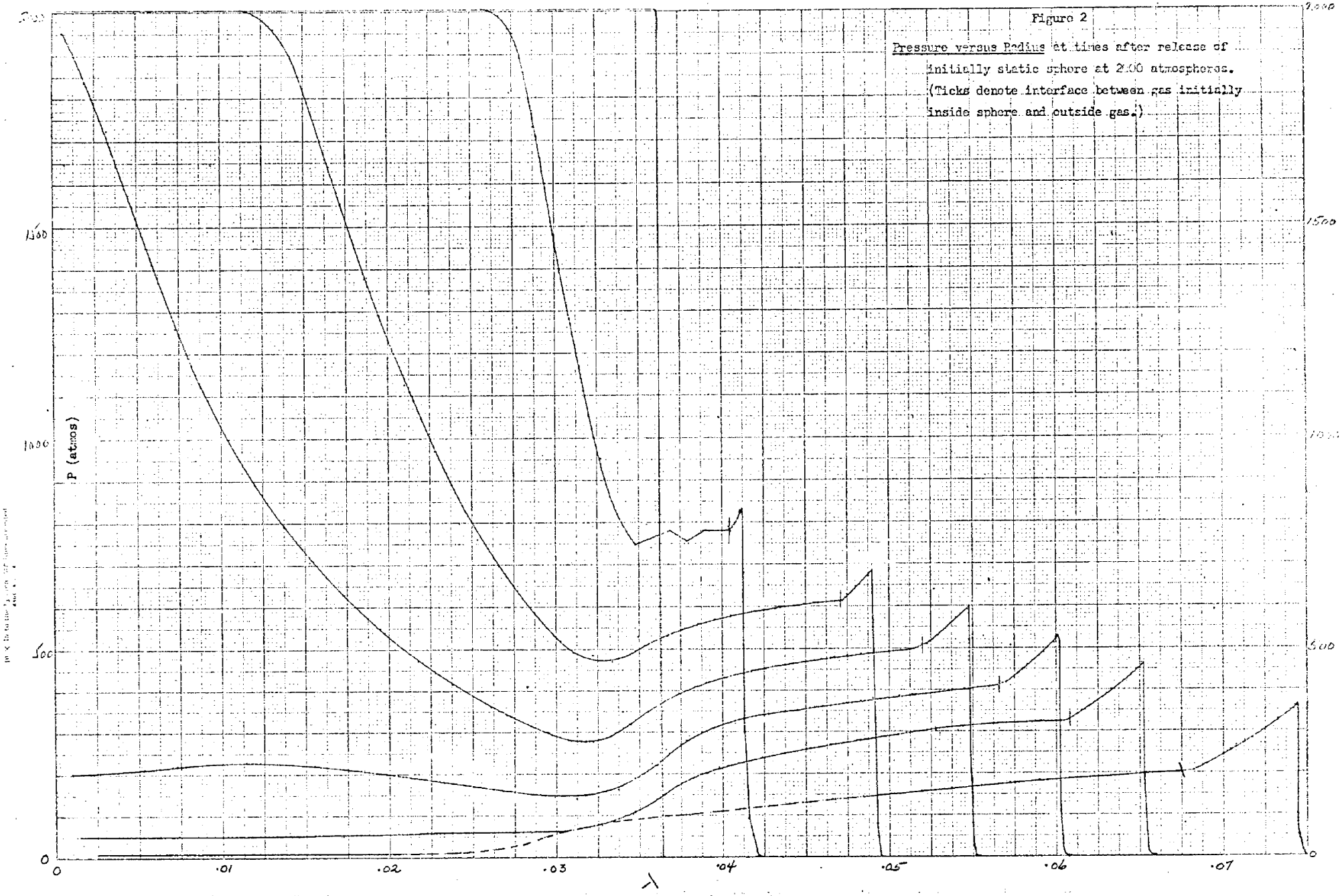

Figure 2

Pressure versus Radius at times after release of initially static sphere at 2000 atmospheres. (Ticks denote interface between gas initially inside sphere and outside gas.)

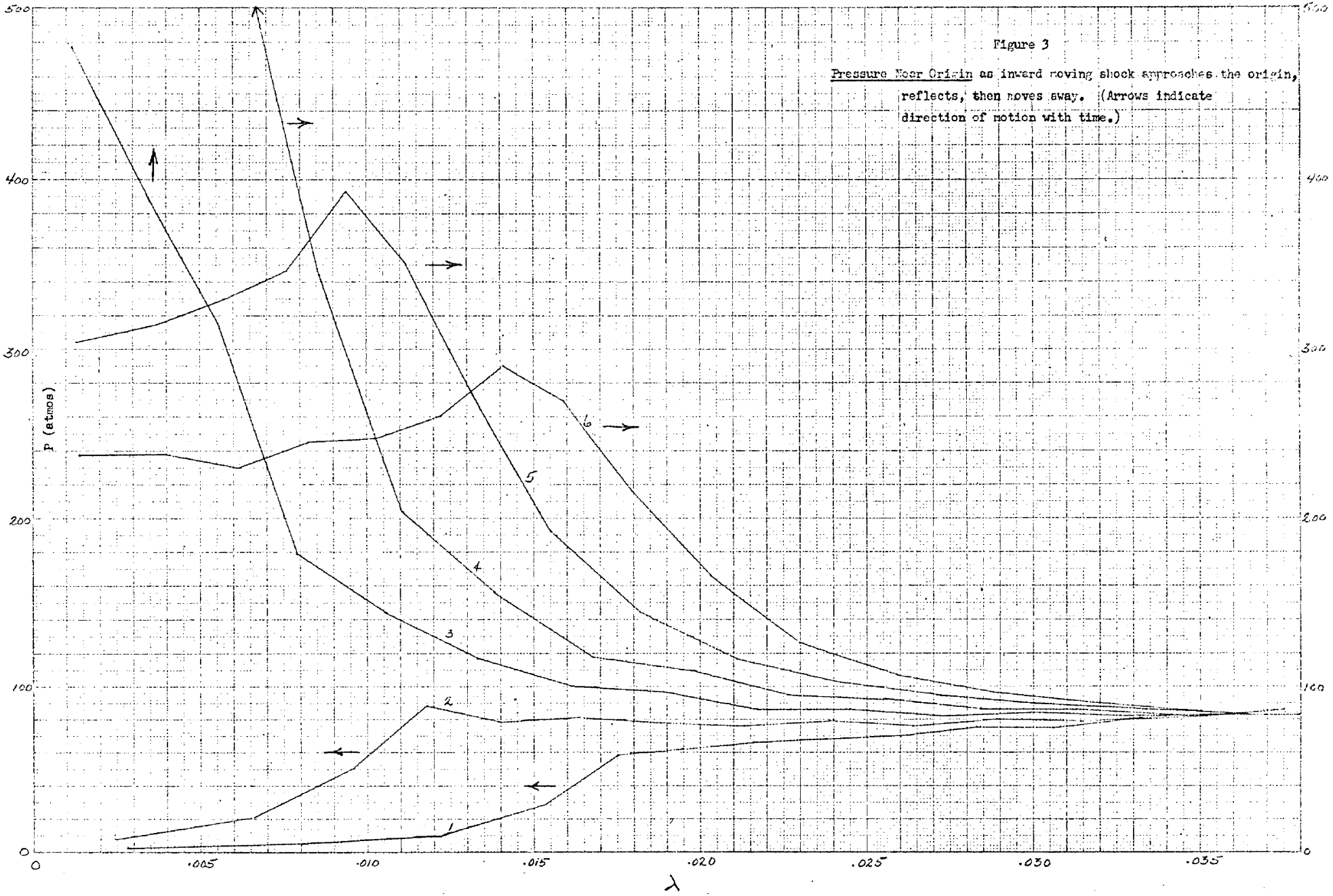

Figure 3

Pressure Near Origin as inward moving shock approaches the origin, reflects, then moves away. (Arrows indicate direction of motion with time.)

Figure 4

PEAK PRESSURE OF FIRST INWARD SHOCK vs SHOCK POSITION

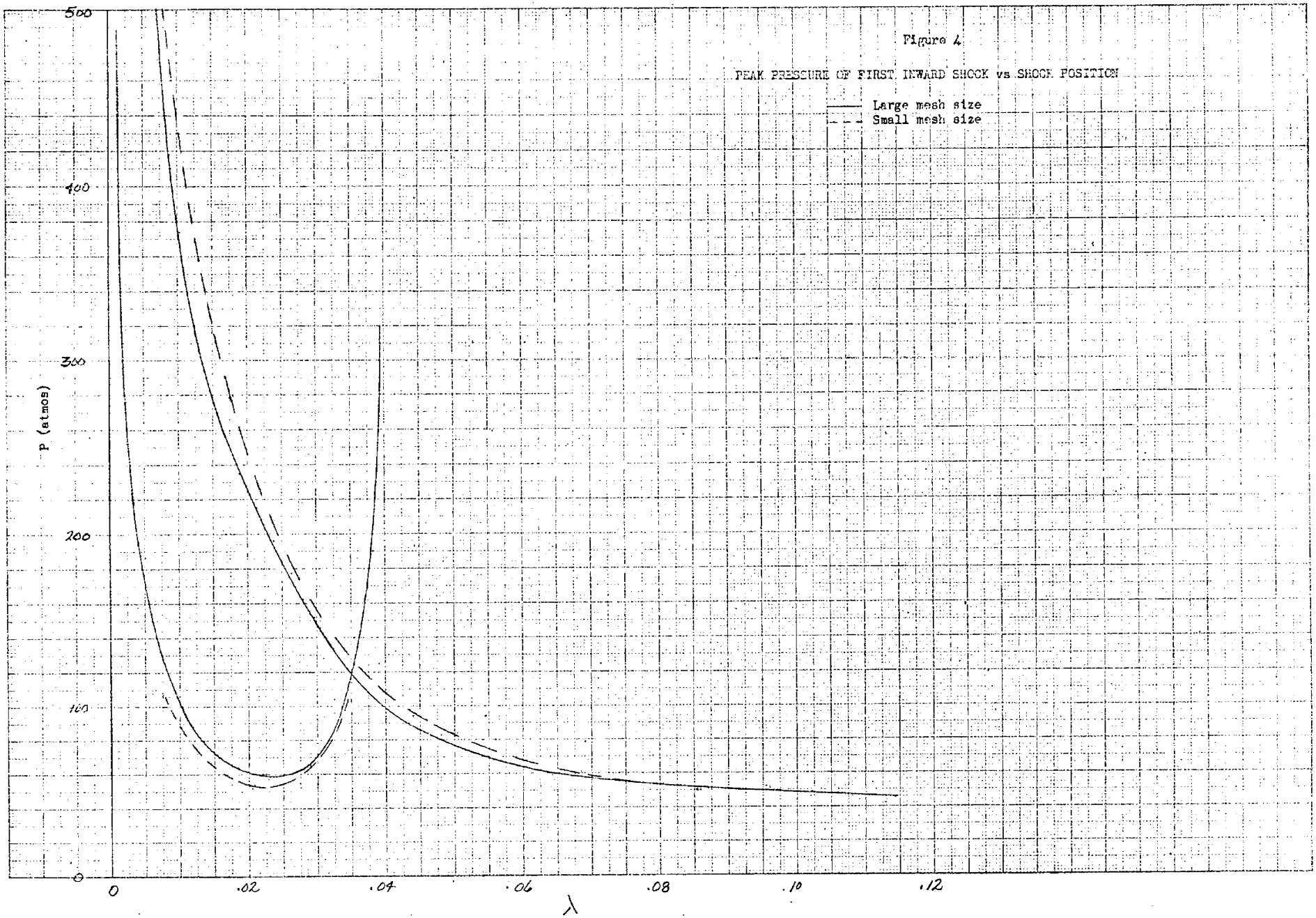

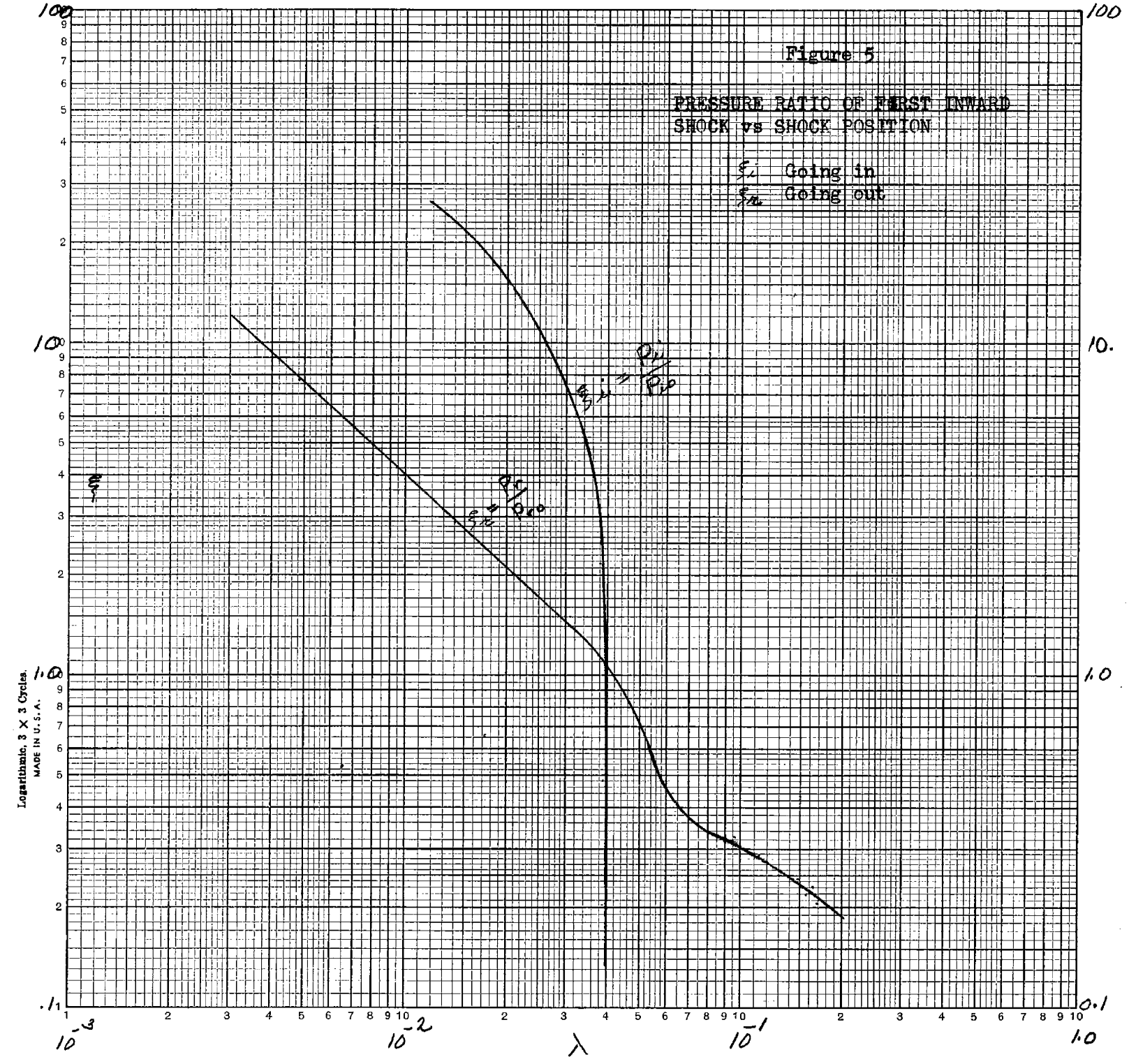
Figure 5
PRESSURE RATIO OF FIRST INWARD SHOCK vs SHOCK POSITION
ξ_i Going in
ξ_o Going out
ξ_i
ξ_o
$\frac{P_s}{P_{s0}}$
$\frac{P_s}{P_{s0}}$
λ
100
10.
1.0
0.1
10^{-3}
10^{-2}
10^{-1}
1.0
Logarithmic, 3 X 3 Cycles.
MADE IN U.S.A.

Figure 6

Density Ratio versus Reduced Radius at various times after release.

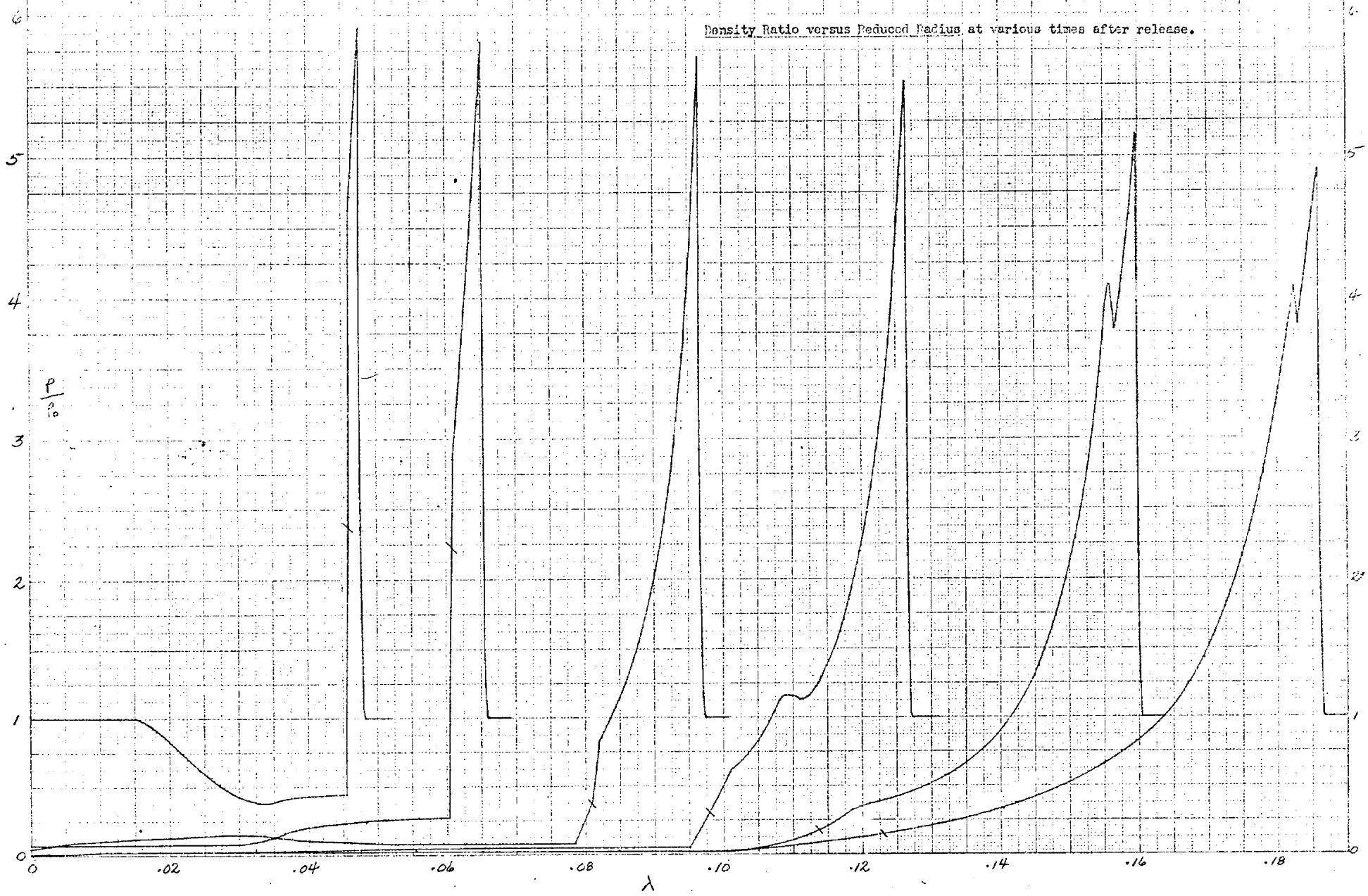

Figure 7

Temperature Ratio versus Reduced Radius at various times after release

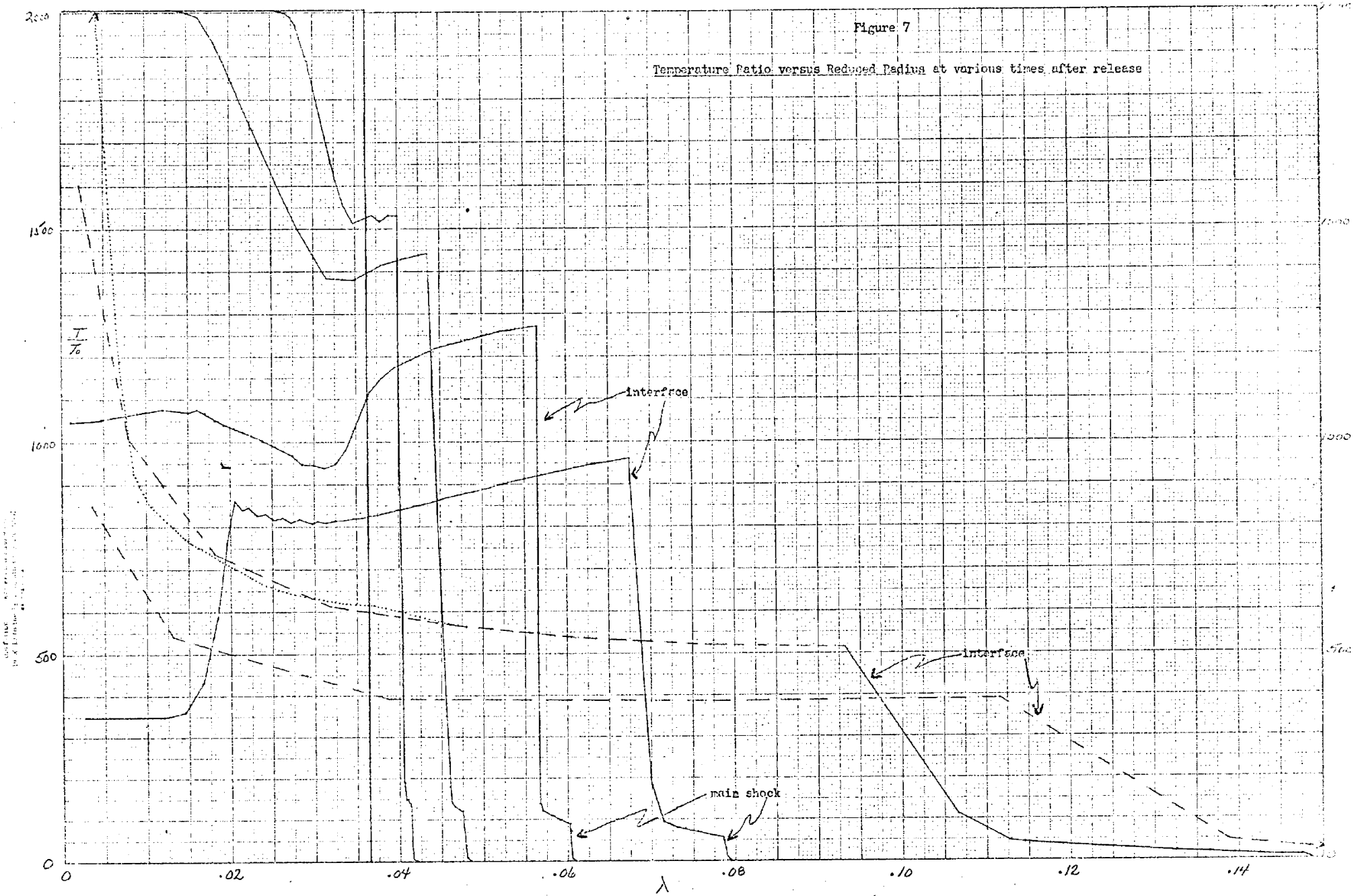

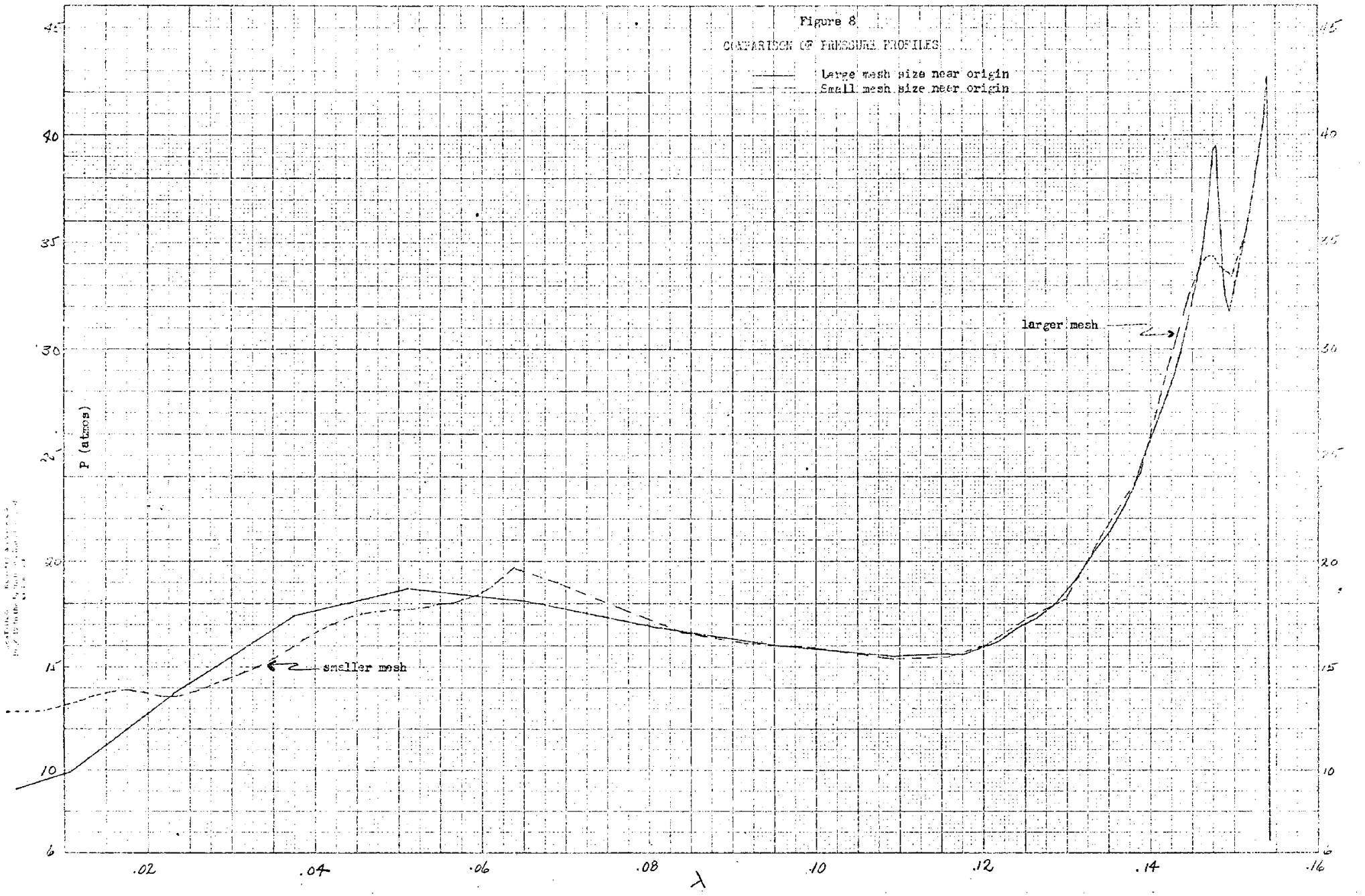
Figure 8
COMPARISON OF PRESSURE PROFILES
Large mesh size near origin
Small mesh size near origin
larger mesh
smaller mesh
P (atmos)
λ
45
40
35
30
25
20
15
10
6
.02
.04
.06
.08
.10
.12
.14
.16

Figure 9

Pressure Profiles Near Center at times when second shock is moving outward through the initial sphere interface. (Ticks mark interface.)

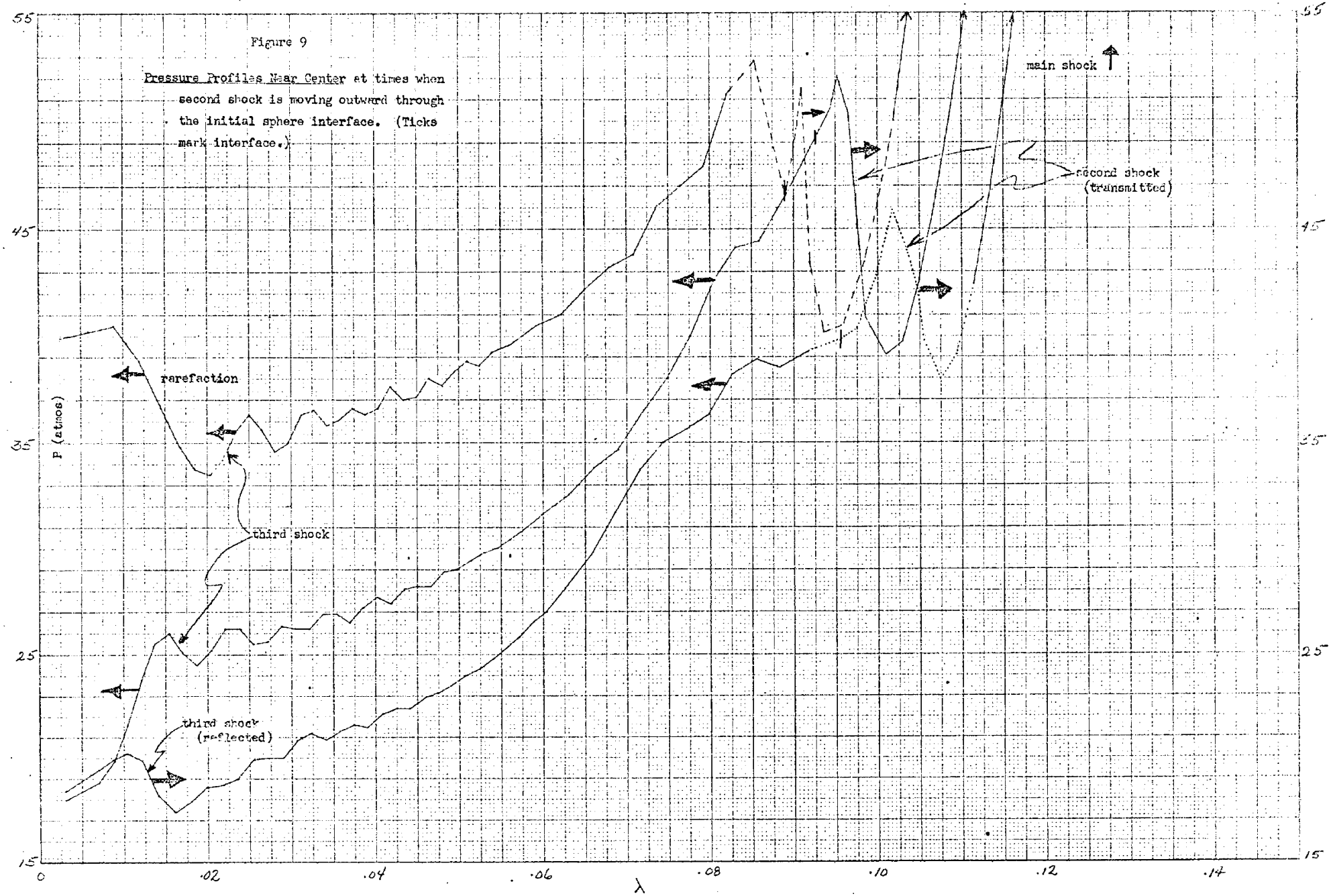

Figure 10

Pressure versus Reduced Radius at times after the second shock reflects at origin and before it overtakes the main shock. (Ticks mark the gas from the sphere interface.)

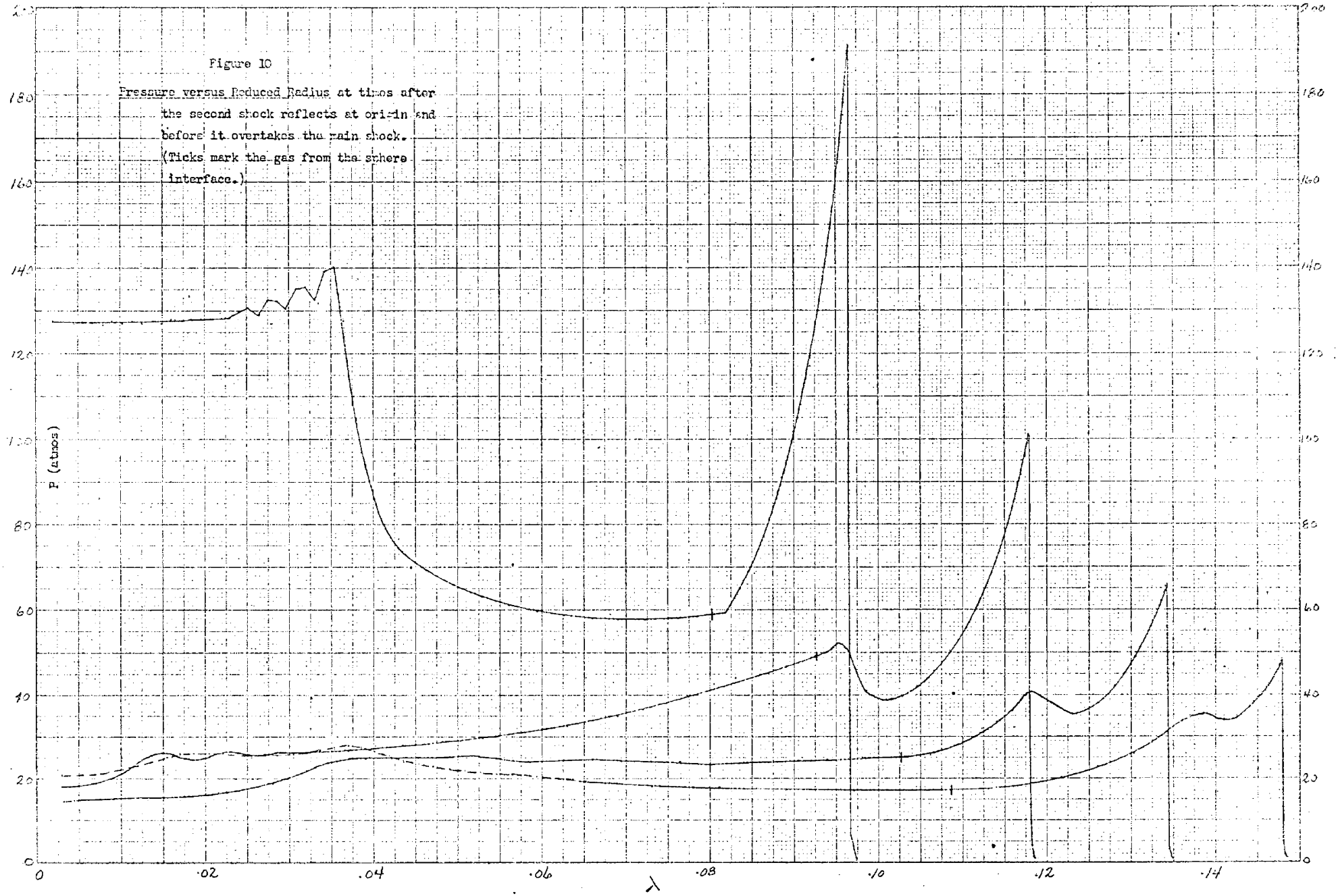

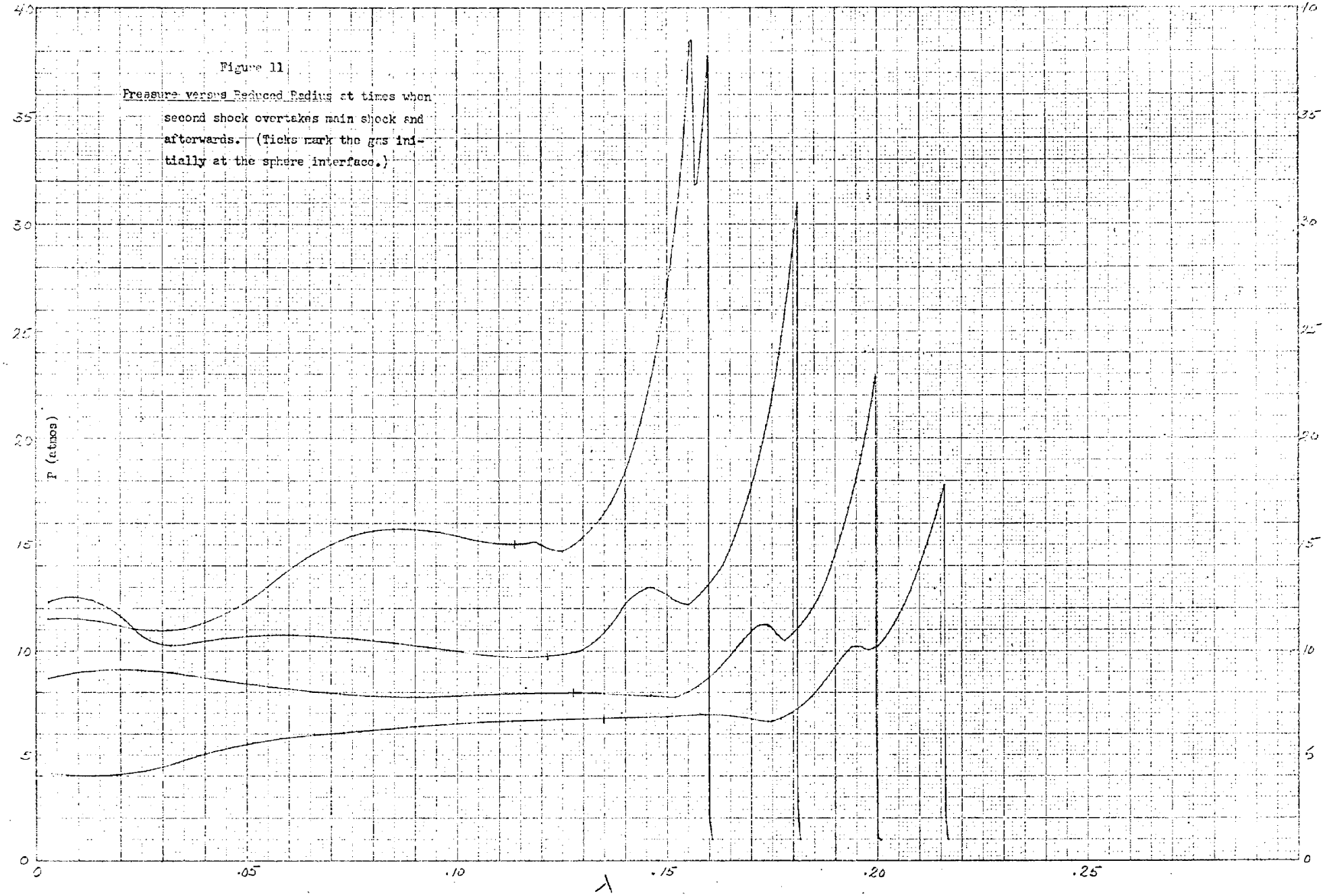

Figure 11

Pressure versus Reduced Radius at times when second shock overtakes main shock and afterwards. (Ticks mark the gas initially at the sphere interface.)